

# **SUPPORTING INFORMATION**

## **Water-Soluble Polymeric Photoswitching Dyads Impart Super Resolution Lysosome Highlighters**

**Chong Li,<sup>#</sup> Zhe Hu,<sup>#</sup> Matthew P. Aldred, Ling-Xi Zhao, Hui Yan, Guo-Feng Zhang, Zhen-Li Huang,<sup>\*</sup> Alexander D. Q. Li,<sup>\*</sup> and Ming-Qiang Zhu<sup>\*</sup>**

### **CONTENTS**

- 1. GPC CURVES OF 10.**
- 2. DYNAMIC LIGHT SCATTERING OF 10.**
- 3. CYCLIZATION REACTION YIELDS CALCULATION.**
- 4. OPTICAL PROPERTIES of DTE-NI AND 10.**
- 5. MTT ASSAY.**
- 6. FLUORESCENCE SWITCHING IMAGING.**
- 7. SUPER-RESOLUTION MICROSCOPY IMAGING.**
- 8. DFT CALCULATION.**
- 9. NMR SPECTRA.**
- 10. MASS SPECTRA.**
- 11. IR SPECTRA.**

## 1. GPC CURVES OF 10.

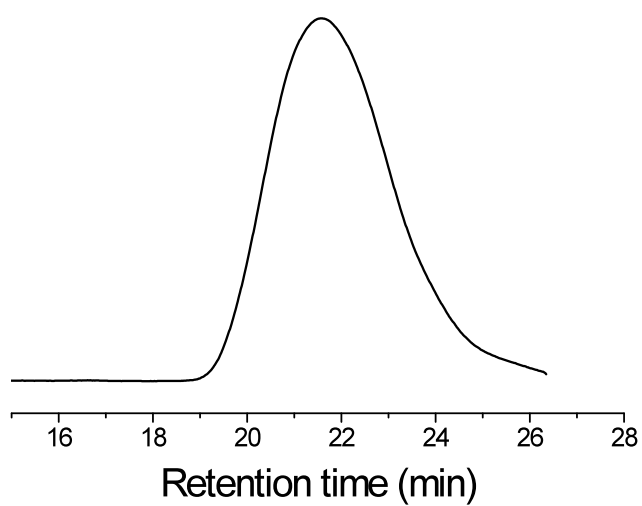


**Figure S1.** GPC curve of Poly[NIPAM-co-(DTE-NI)] eluting with DMF/LiBr.

## 2. DYNAMIC LIGHT SCATTERING OF 10.

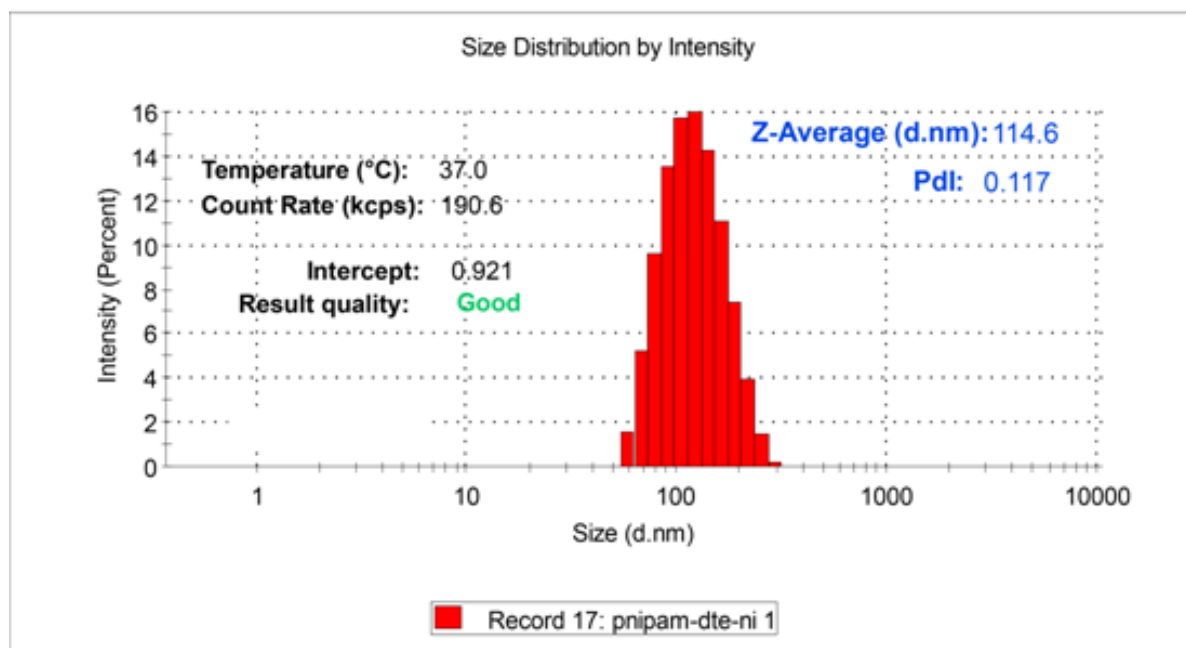


**Figure S2.** Dynamic light scattering of **10** in aqueous solution (1 mg/mL) determined that the Z-average hydrodynamic diameter was 114.6 nm (PD1 = 0.117) at 37°C for the aggregated polymers. At 25°C, there is no observable signal because **10** molecules are hydrophilic and dispersed in the aqueous solution as free macromolecules with a theoretical hydrodynamic diameter of several nanometers.

### 3. CYCLIZATION REACTION YIELDS CALCULATION.

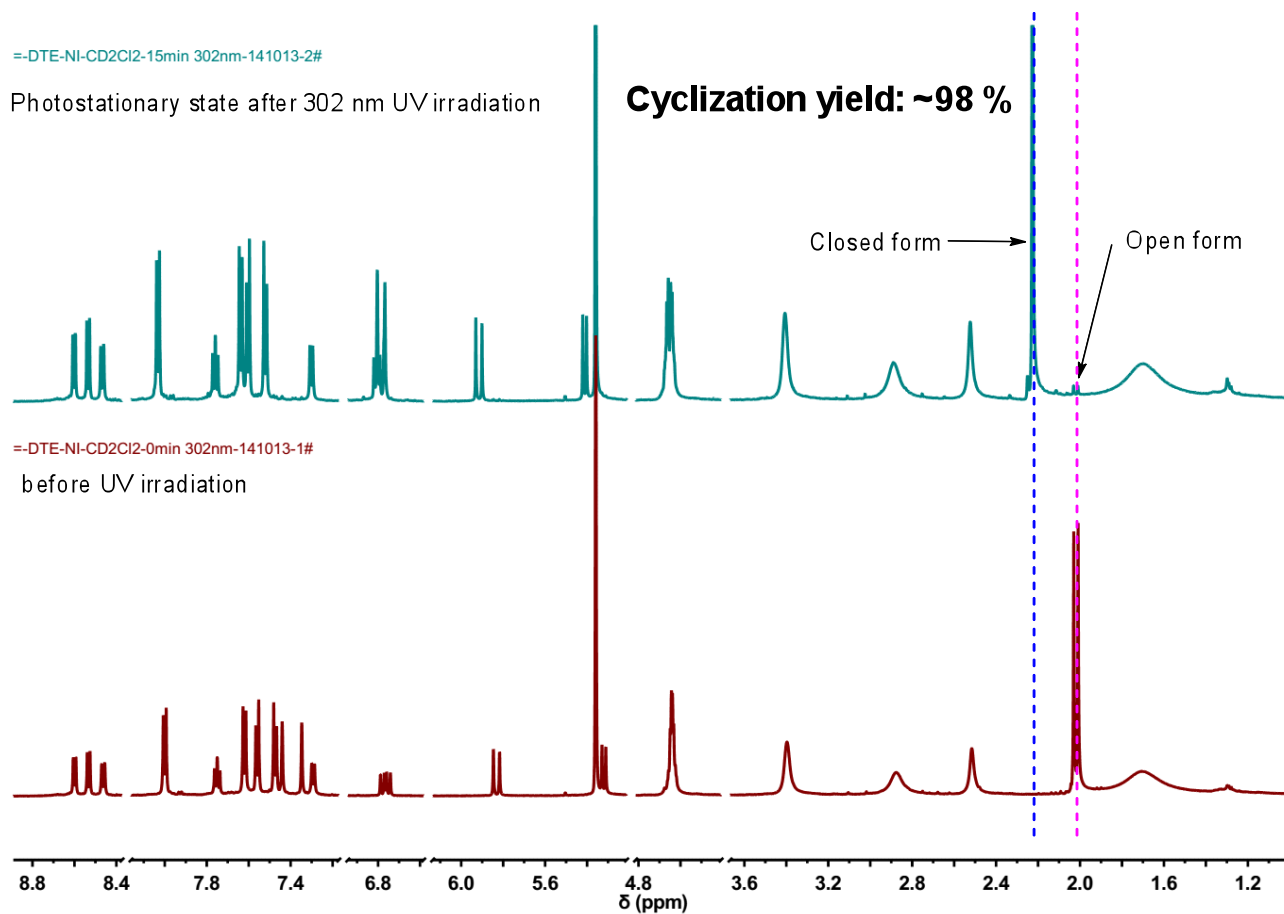
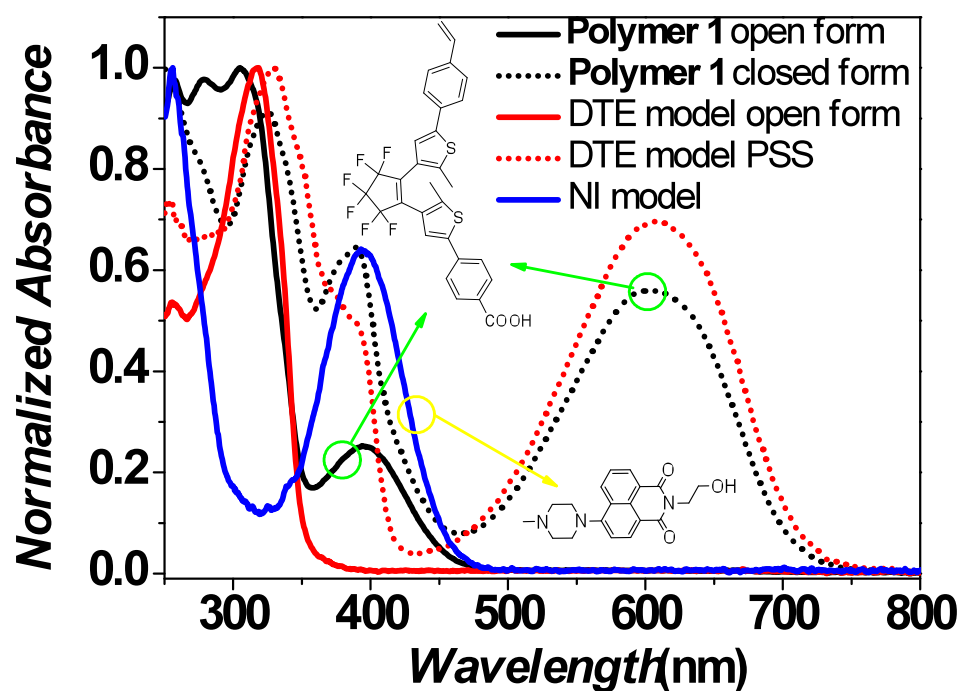
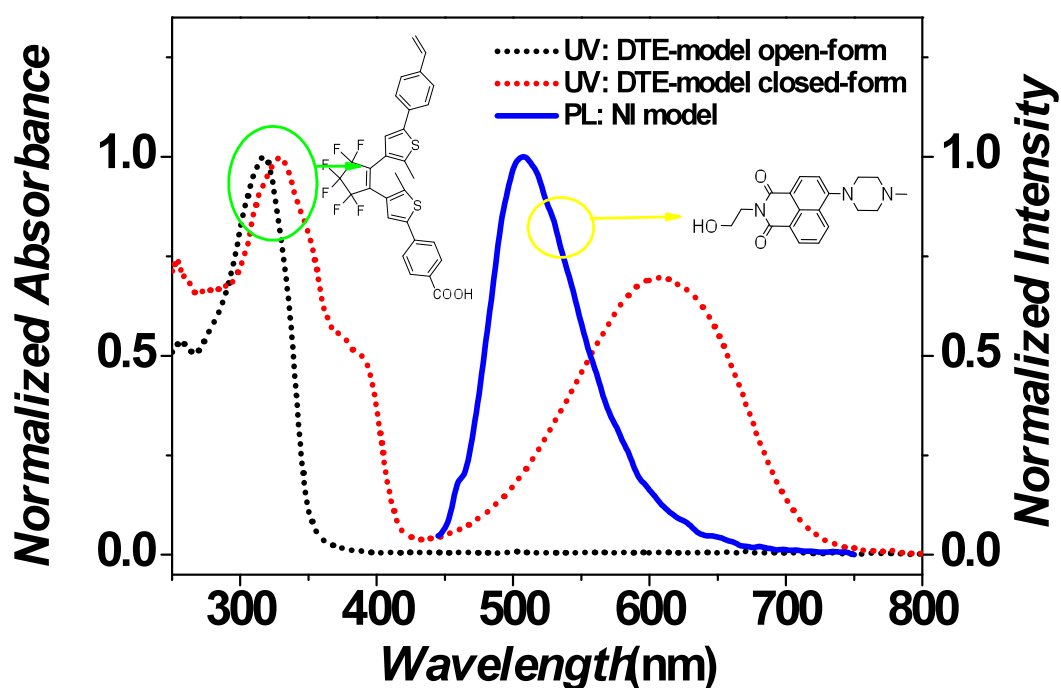


**Figure S3.** The cyclization yield calculation from  $^1\text{H}$  NMR spectra before and after UV irradiation. The chemical shifts of  $-\text{CH}_3$  groups on thiophene rings of open-form DTE distinguished significantly from that of closed-form DTE. The proportion of integral values of  $-\text{CH}_3$  groups on closed-form DTE in PSS represents the cyclization yield (98% for 302 nm UV irradiation). The solvent is  $\text{CD}_2\text{Cl}_2$ .

#### 4. OPTICAL PROPERTIES of DTE-NI AND 1O.



(a)



(b)

**Figure S4.** The comparison of absorption and emission spectra of compound **8** (model DTE), compound **9** (model NI) and polymer **1** in THF solution. a) Absorption spectra for all in the same scale. b) The emission spectrum of model NI overlaps significantly with the closed-form model DTE.

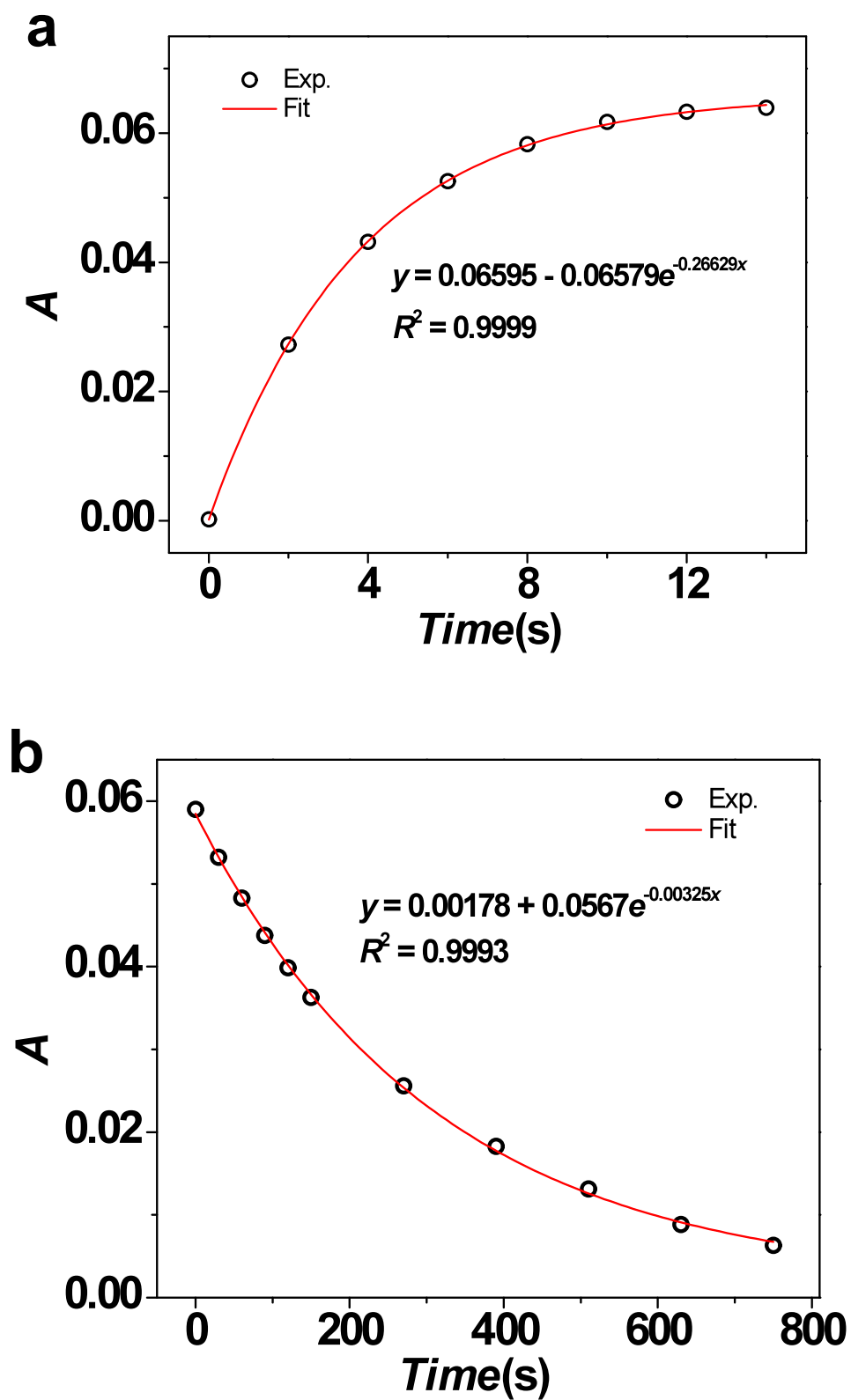


**Figure S5.** The photo-kinetics curves of monomer **DTE-NI** upon (a) 302-nm UV irradiation (2.76 mW/cm<sup>2</sup>) and (b) followed by 617-nm LED light irradiation (3.54 mW/cm<sup>2</sup>). The experimental absorbance data at 600 nm (circles) are fitted to a monoexponential function (red line). The obtained rate constants are used for photoisomerization quantum yields calculation.

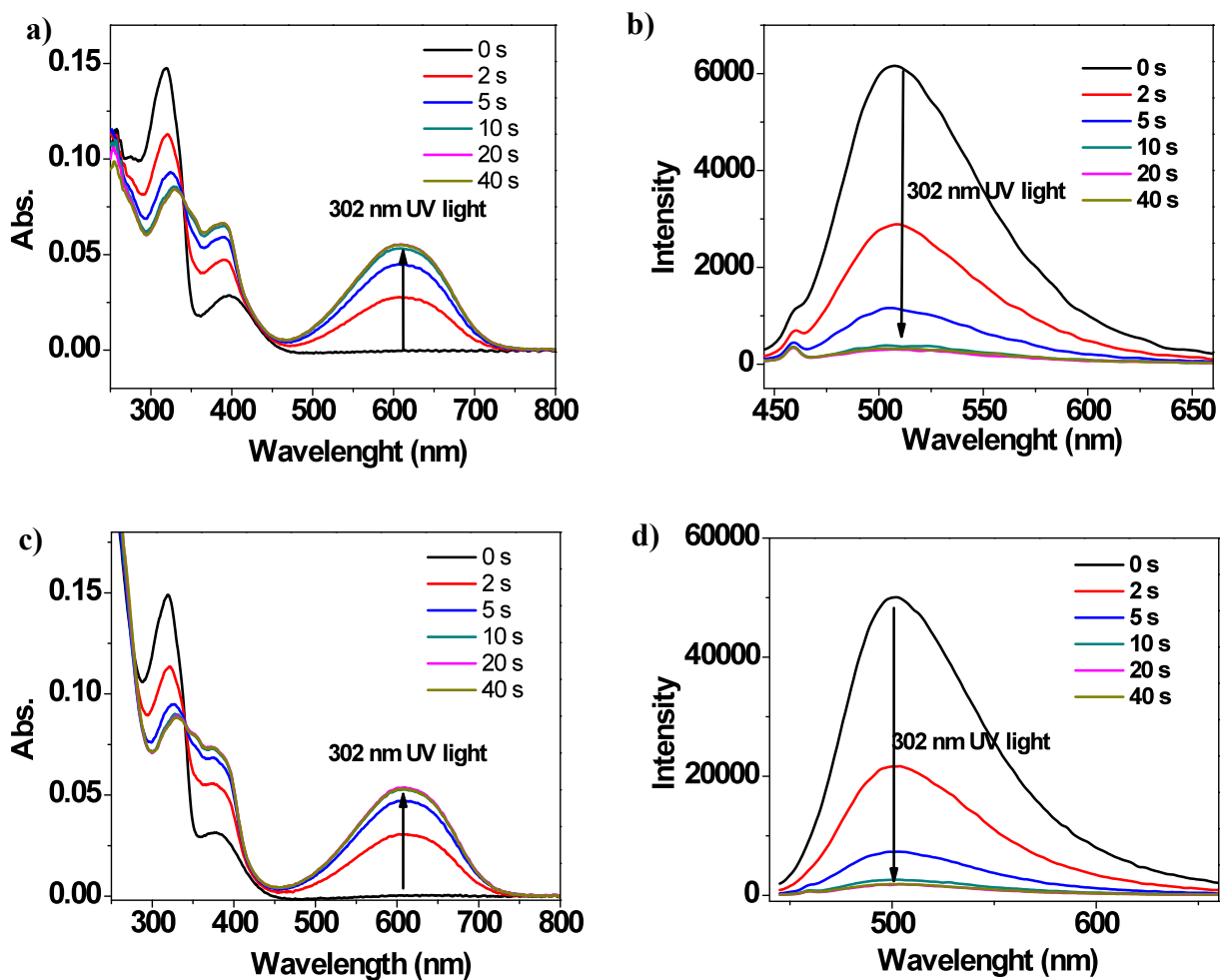


**Figure S6.** UV-Vis Absorption and emission spectra of **DTE-NI** upon 302 nm irradiation. a) and b) in THF; c) and d) in THF with one drop 2 M aq. HCl (pH is about 2 tested by pH indicator paper). Concentration =  $3 \times 10^{-6}$  M. Excitation = 405 nm.

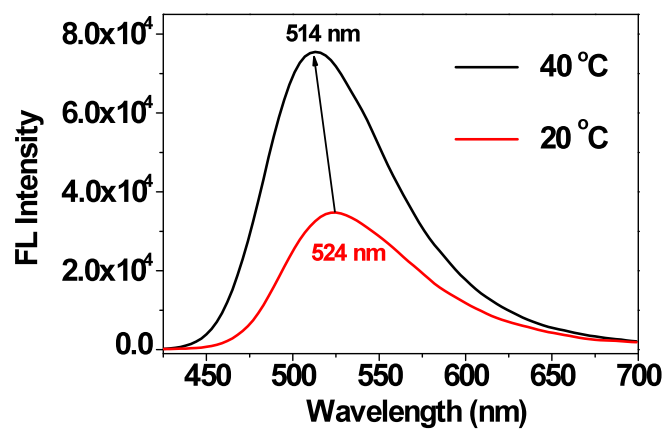


**Figure S7.** Temperature-dependent emission spectra of polymer **1** in aqueous solutions. Concentration = 1.0 mg/mL. Excitation = 440 nm.



**Scheme S1.** The mechanism of pH sensitive fluorescence of polymer 1.

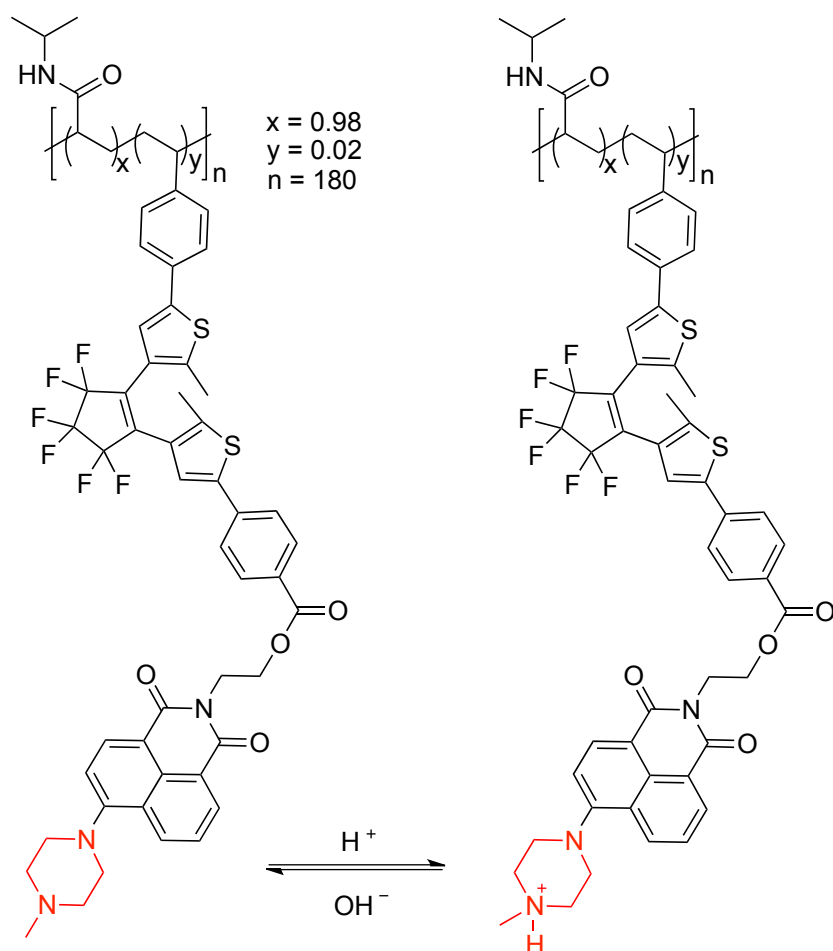
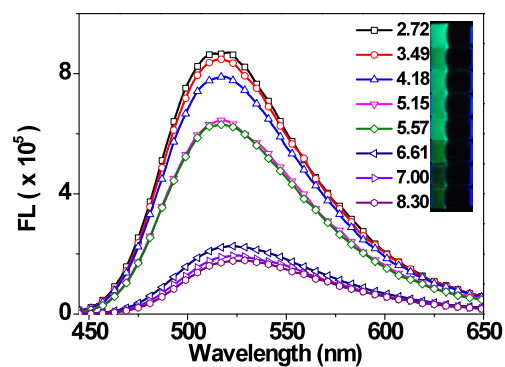


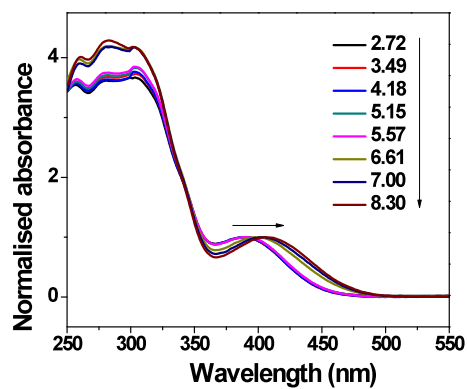
**Table S1** Relative fluorescent quantum yields ( $\Phi_F$ ) of Poly[NIPAM-co-(DTE-NI)] at different pH values

pH	2.72	3.48	4.18	5.15	5.57	6.61	7.00	8.30
$\lambda_{\text{max,abs}}$	388.5	389.0	389.0	389.5	390.5	398.5	405.0	405.5
$\lambda_{\text{max,PL}}$	514.0	516.0	518.0	518.0	517.0	522.0	525.0	527.0
$\Phi_F$	14.5%	14.2%	13.2%	10.7%	10.5%	3.9%	3.3%	3.0%

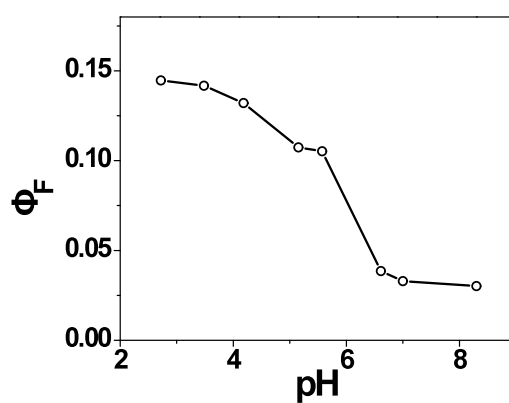
$\lambda_{\text{max,abs}}$  is the lowest energy absorption peak.  $\lambda_{\text{max,PL}}$  is the emission peak measured at excitation= 514 nm.  $\Phi_F$  is the fluorescence quantum yields relative to 4-(dicyanomethylene)-2-methyl-6-(p-dimethylaminostyryl)-4H-pyran (43.5 % in ethanol). <sup>1</sup> The excitation wavelength for  $\Phi_F$  is 440 nm.



(a)

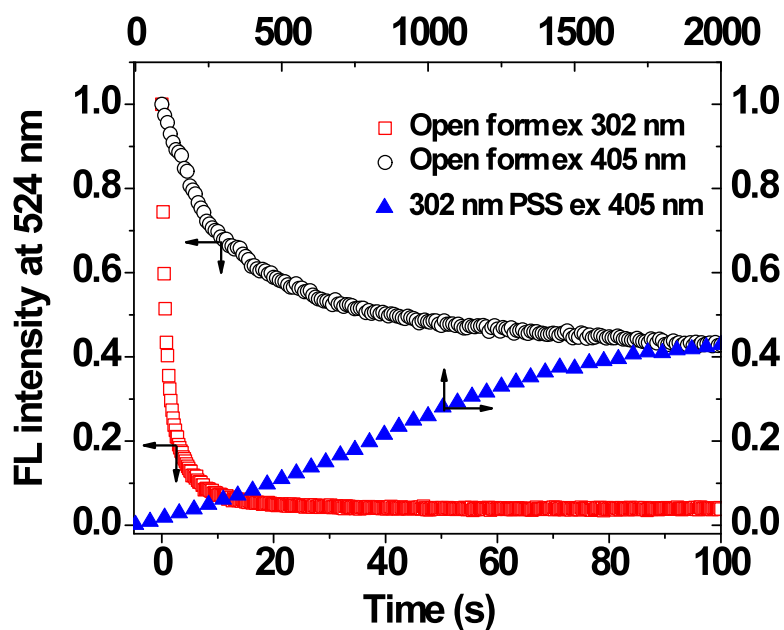


(b)

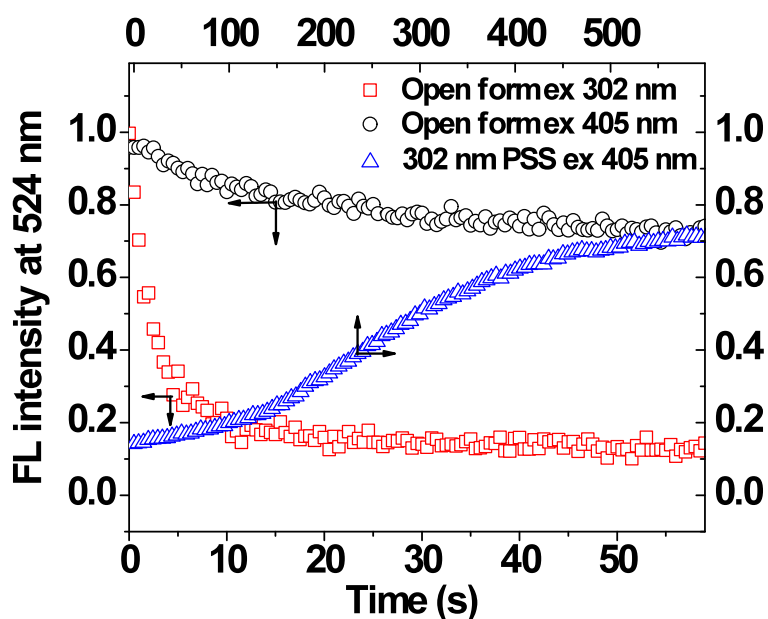


(c)

**Figure S8.** pH-sensitive emission spectra (a), absorption spectra (b) and quantum yields (c) of polymer **1** in aqueous solutions with different pH values (acetic acid- sodium acetate buffer). Concentration = 1.0 mg/mL. Excitation = 440 nm.

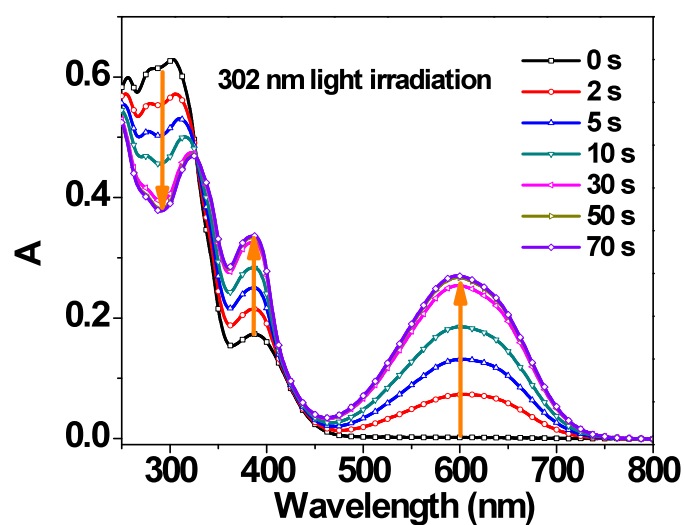


(a)

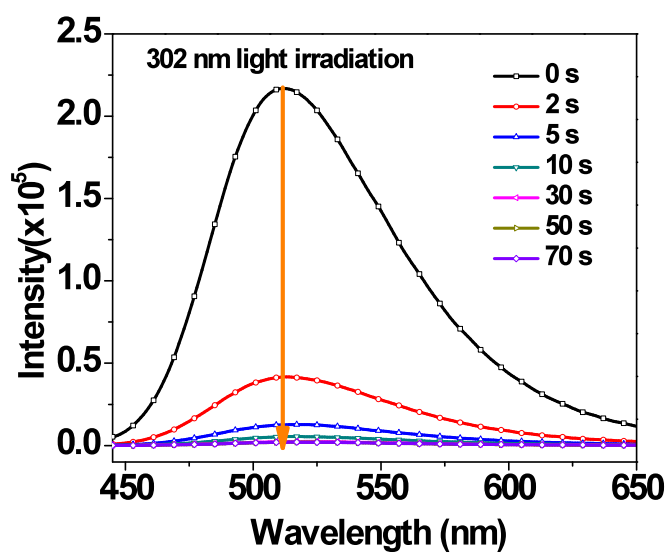


(b)

**Figure S9.** Excitation wavelength-dependent changes of emission intensity at maximum emission wavelength 524 nm. a) pH = 3, b) pH = 7. Red line is the emission change of **1O** excited at 302 nm; black line is the emission change of **1O** excited at 405 nm; blue line is the emission change of **1C** (photostationary state at 302 nm UV irradiation) excited at 405 nm. The concentration is 1.0 mg/mL in water.



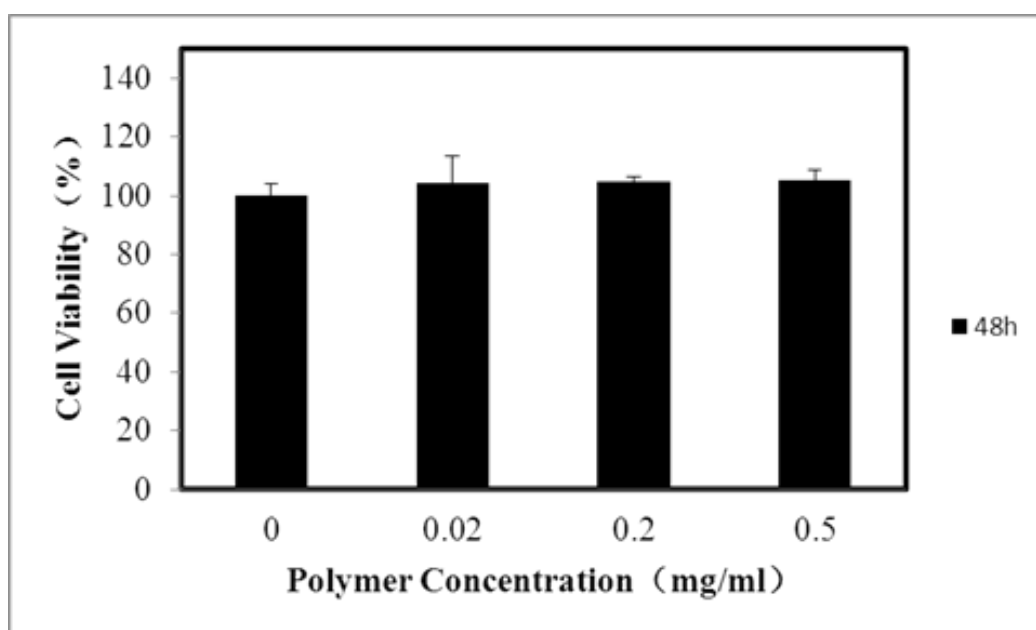
(a)



(b)

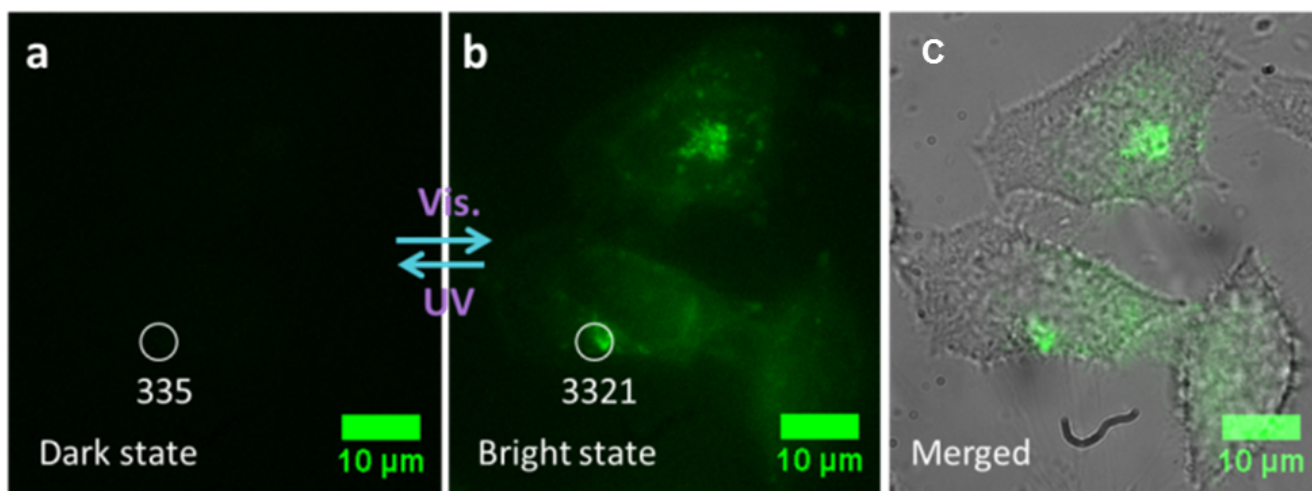
**Figure S10.** The changes in the UV/Vis absorption (a) and emission spectra (b) of polymer **1** in pH=3 aqueous solution upon 302 nm irradiation at different time intervals. The concentration of **1** is 1.0 mg/mL and the excitation wavelength is 440 nm.

## 5. MTT ASSAY



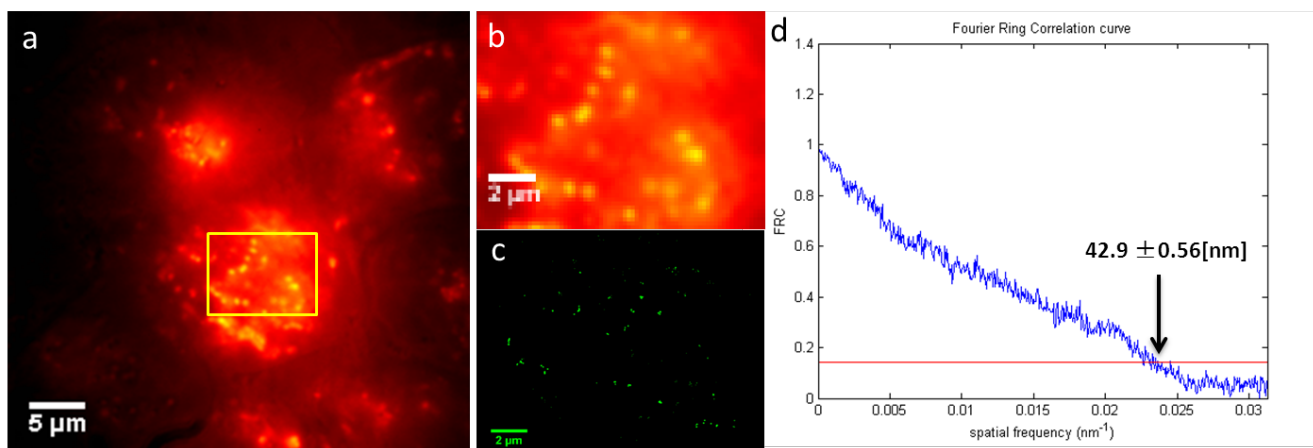
**Figure S11.** MTT assay of polymer **1** in HeLa cell incubated for 48h.

## 6. FLUORESCENCE SWITCHING IMAGING.

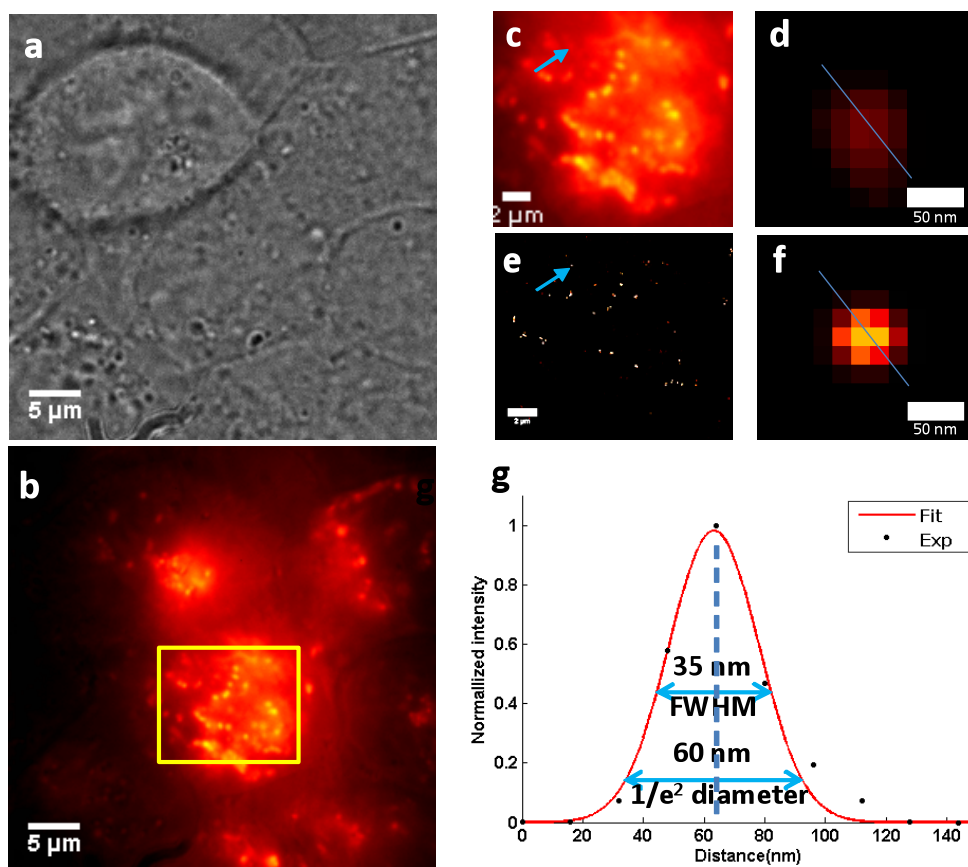


**Figure S12.** Fluorescence switching of HeLa living cells incubated with polymer 1 for 24 h at 37 °C by alternating UV (302 nm,  $\sim 0.4$  mW/cm<sup>2</sup>) and visible (405 nm,  $\sim 10$  W/cm<sup>2</sup>) light illumination. (a) irradiated by 302 nm light (b) irradiation with strong 405 nm light (c) the merged image of bright-field and bright state. The excitation wavelengths were the same weak 405 nm light for all images. The inseted numbers in (a) and (b) are the highest intensity value of circled region.

## 7. SUPER-RESOLUTION MICROSCOPY IMAGIN

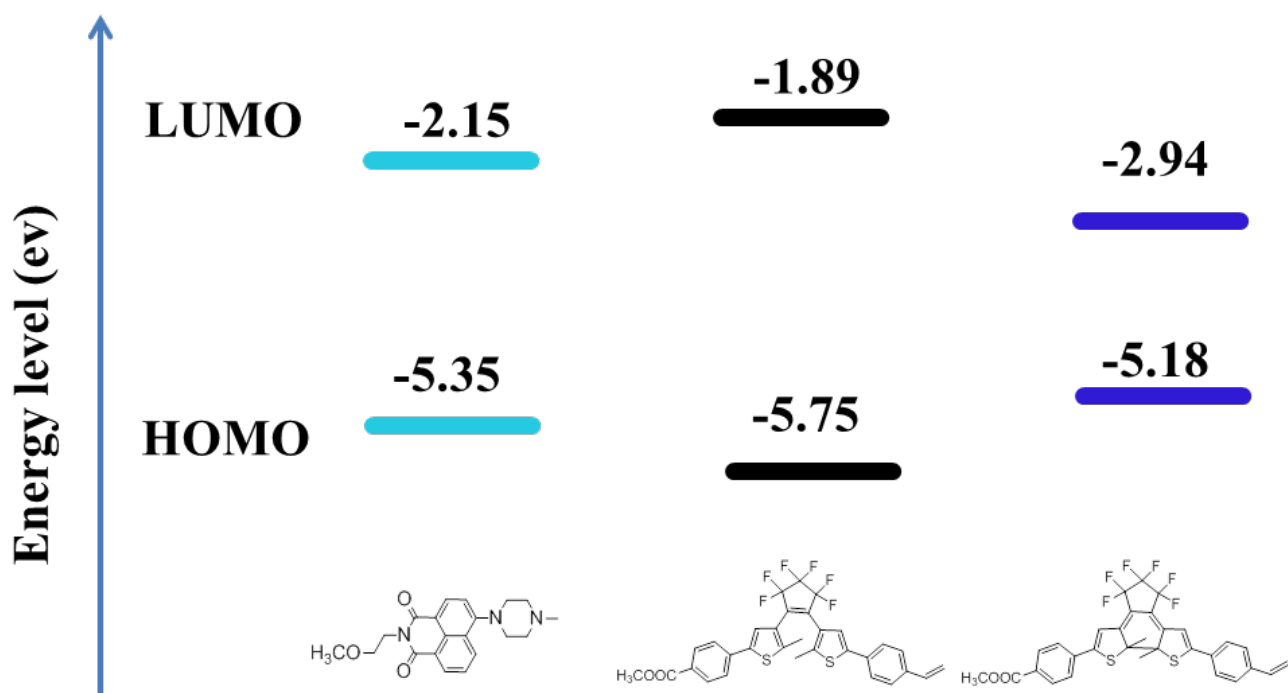


**Figure S13.** Spatial resolution calculation; (a) conventional fluorescent image displaying the distribution of **1O**, (b) expanded view and conventional fluorescent image of the yellow box marked regions in (a), (c) super-resolution fluorescent image of the yellow box marked regions in (a), (d) fourier ring correlation curve calculated from (b) and (c).



**Figure S14** Super-resolution imaging of **1O**- labeled HeLa cells; (a) bright-field image. (b) conventional fluorescent image displaying the distribution of **1O**. (c) expanded view and conventional fluorescent image of the yellow box marked regions in (b). (e) super-resolution fluorescent image of the yellow box marked regions in (b). (d) and (f) expanded view of the arrow pointed spot in (c) and (e), respectively. (g) fluorescence cross-sectional profiles of a **1O** fluorescence spot along the dashed lines in (f), indicating FWHM (full width at half maximum) width and the  $1/e^2$  diameter of the localized polymer probes to be 35 nm and 60 nm respectively.

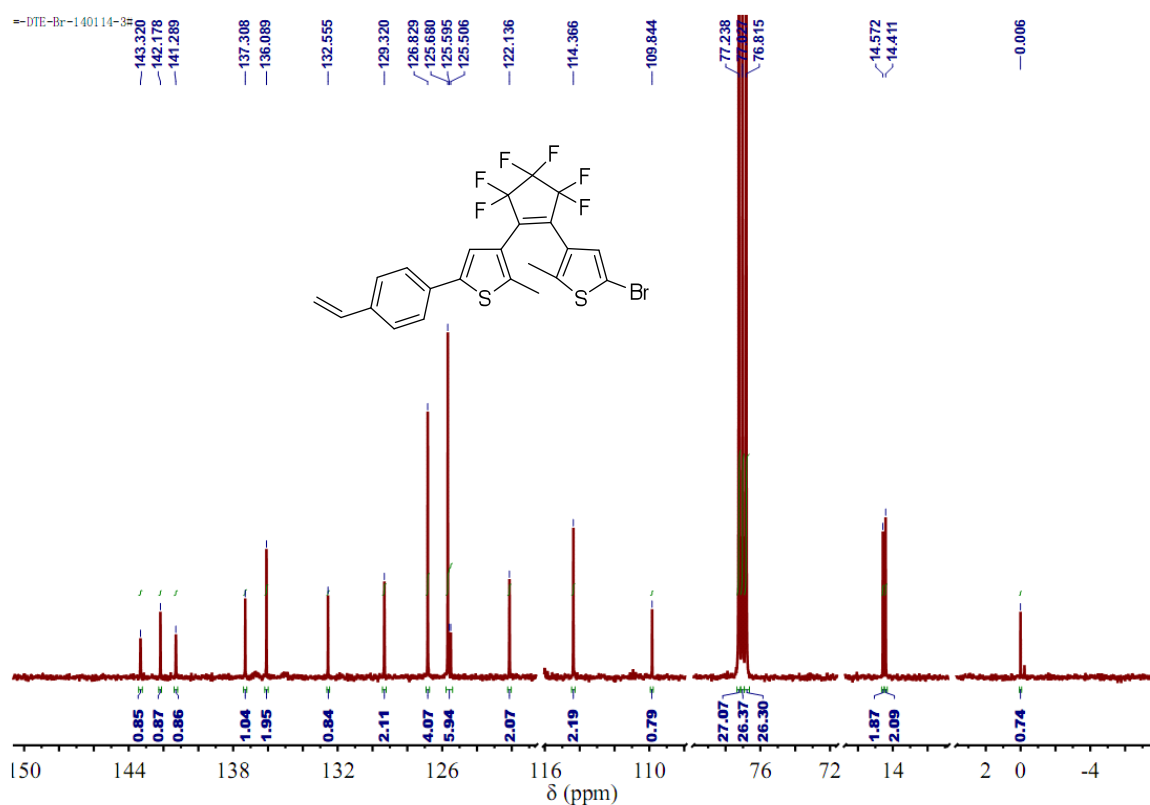
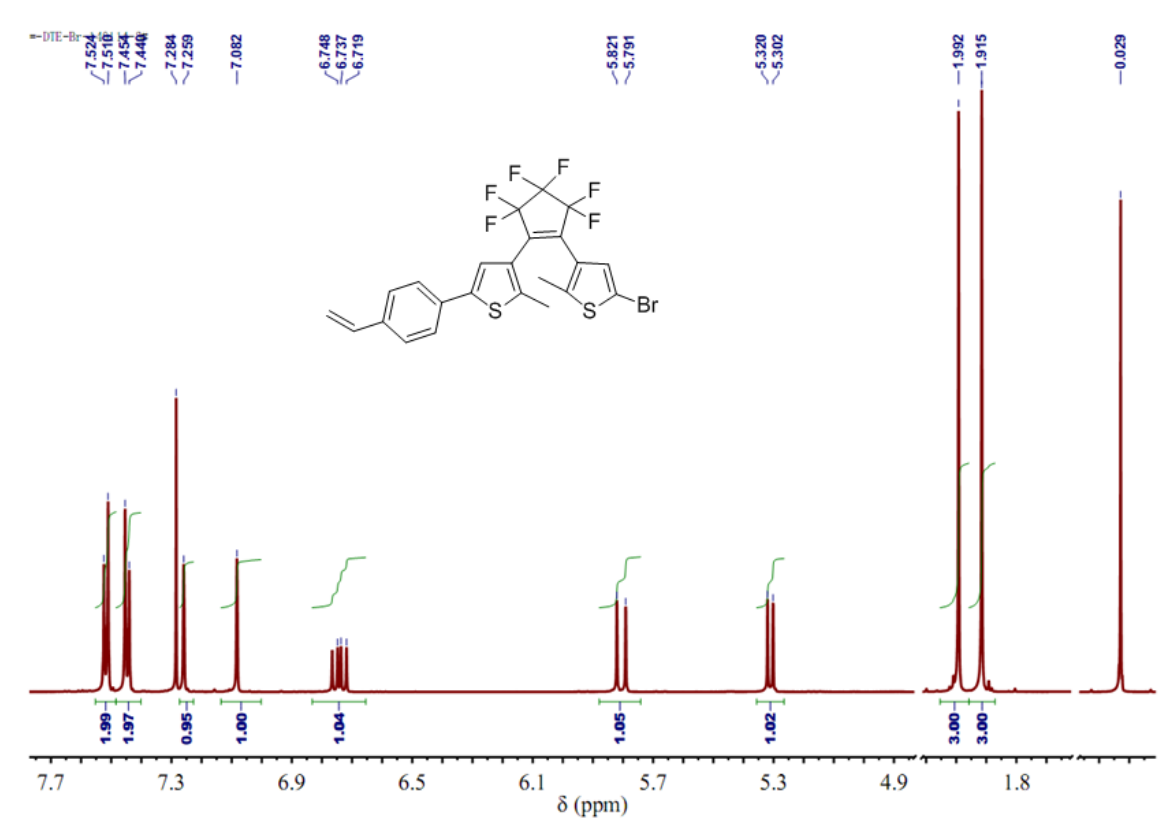
## 8. DFT CALCULATION.

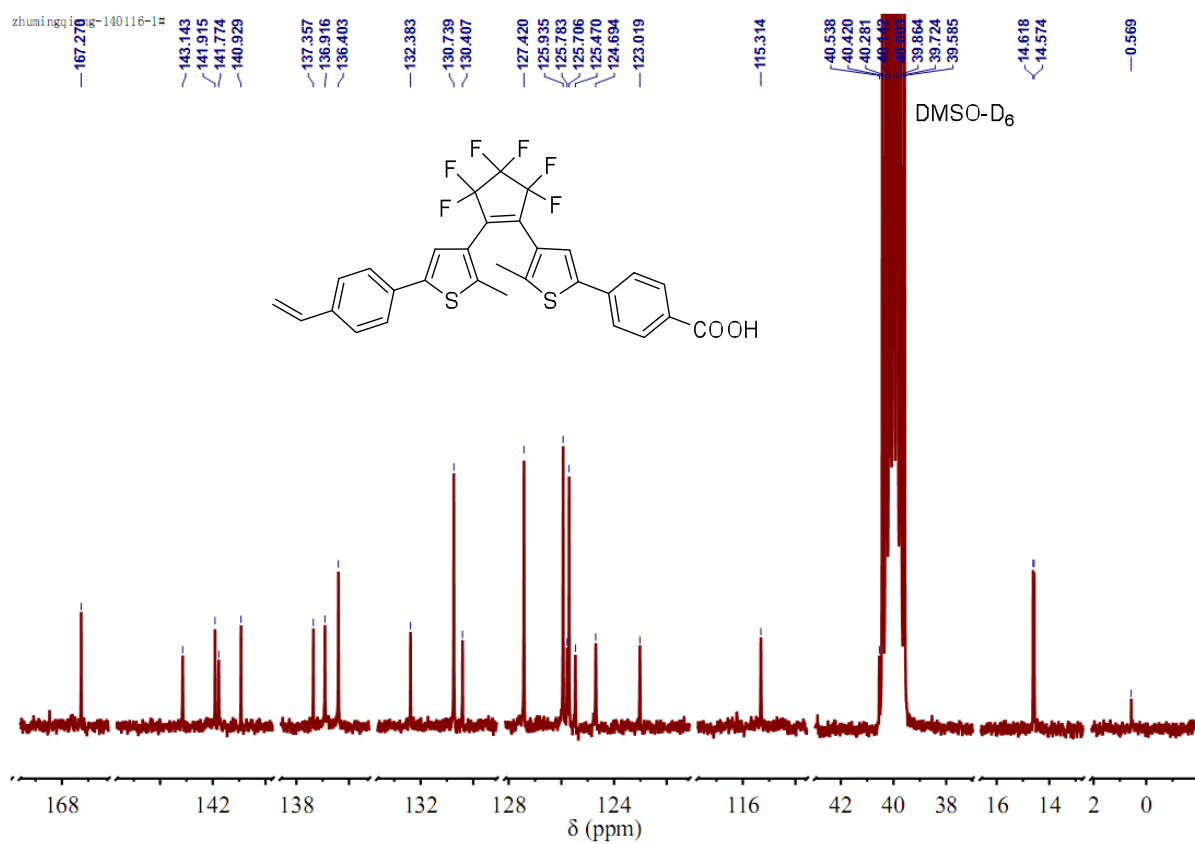
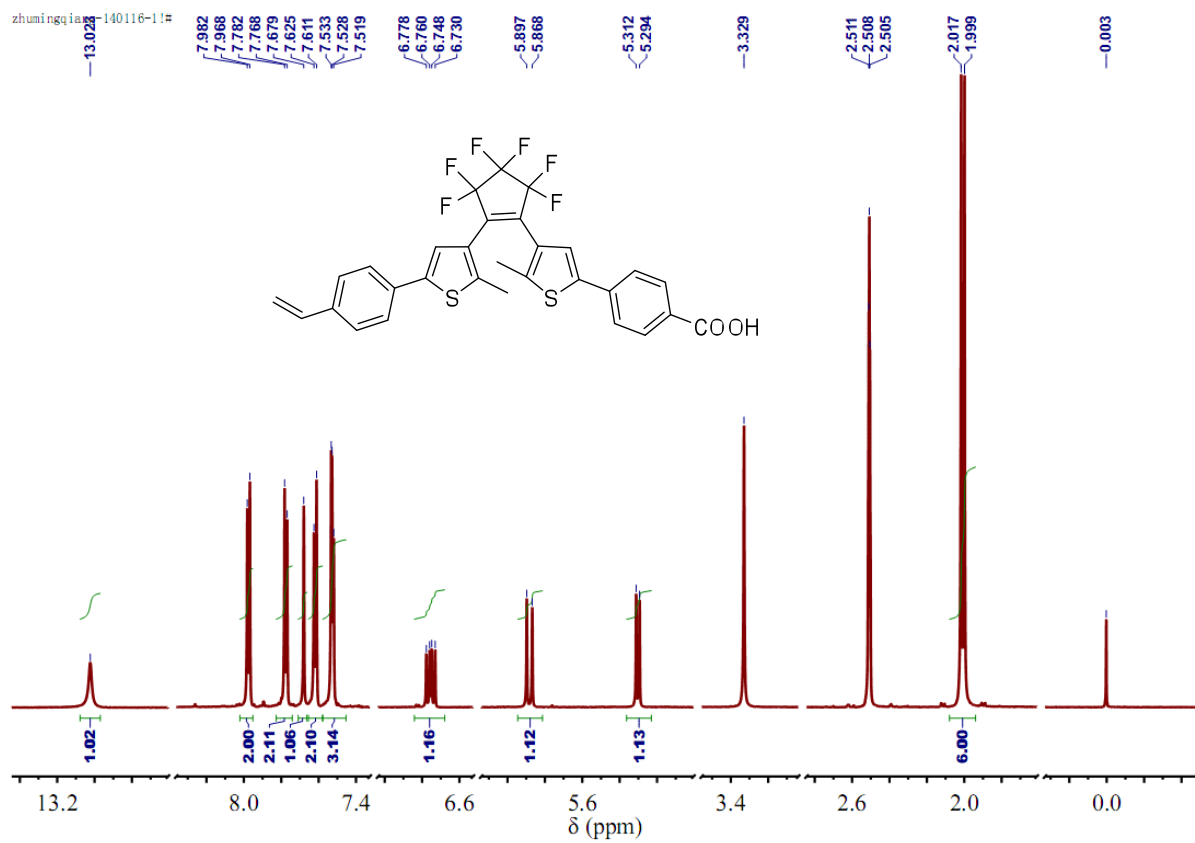


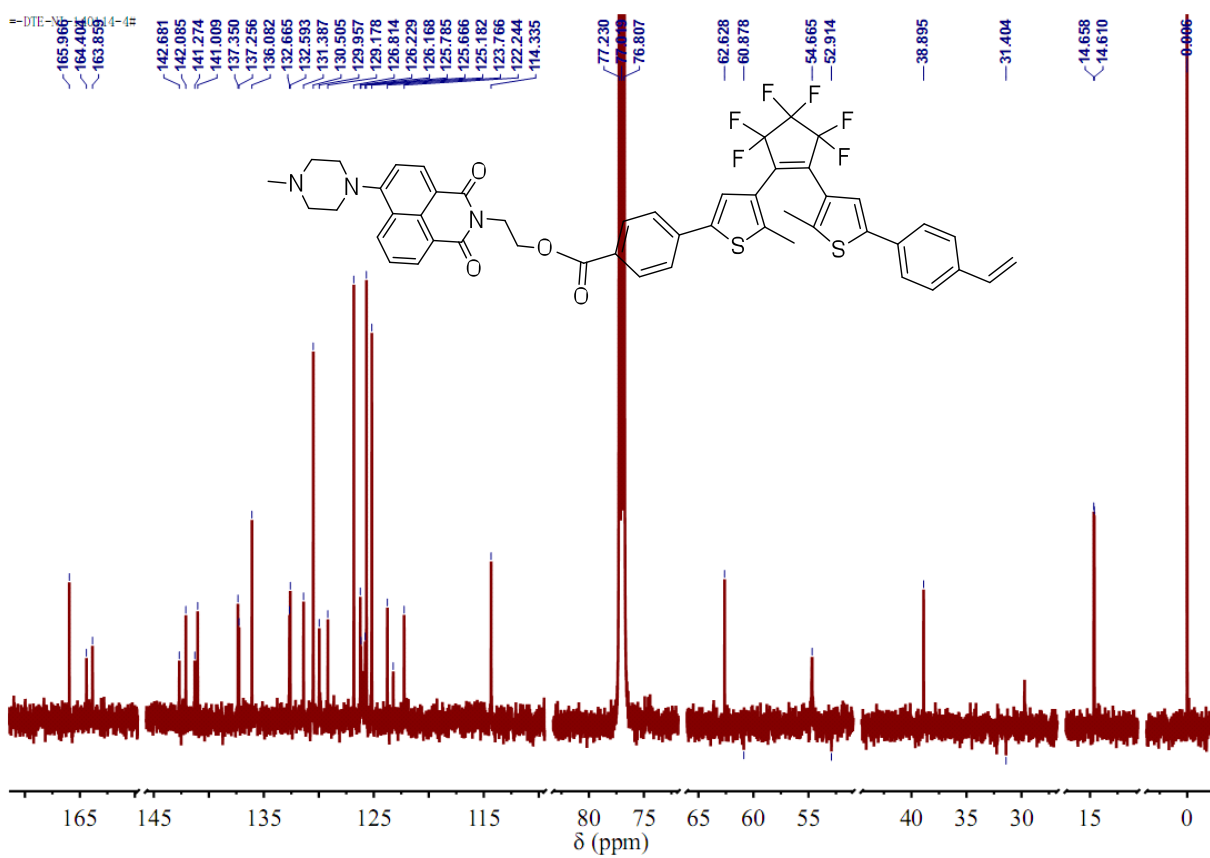
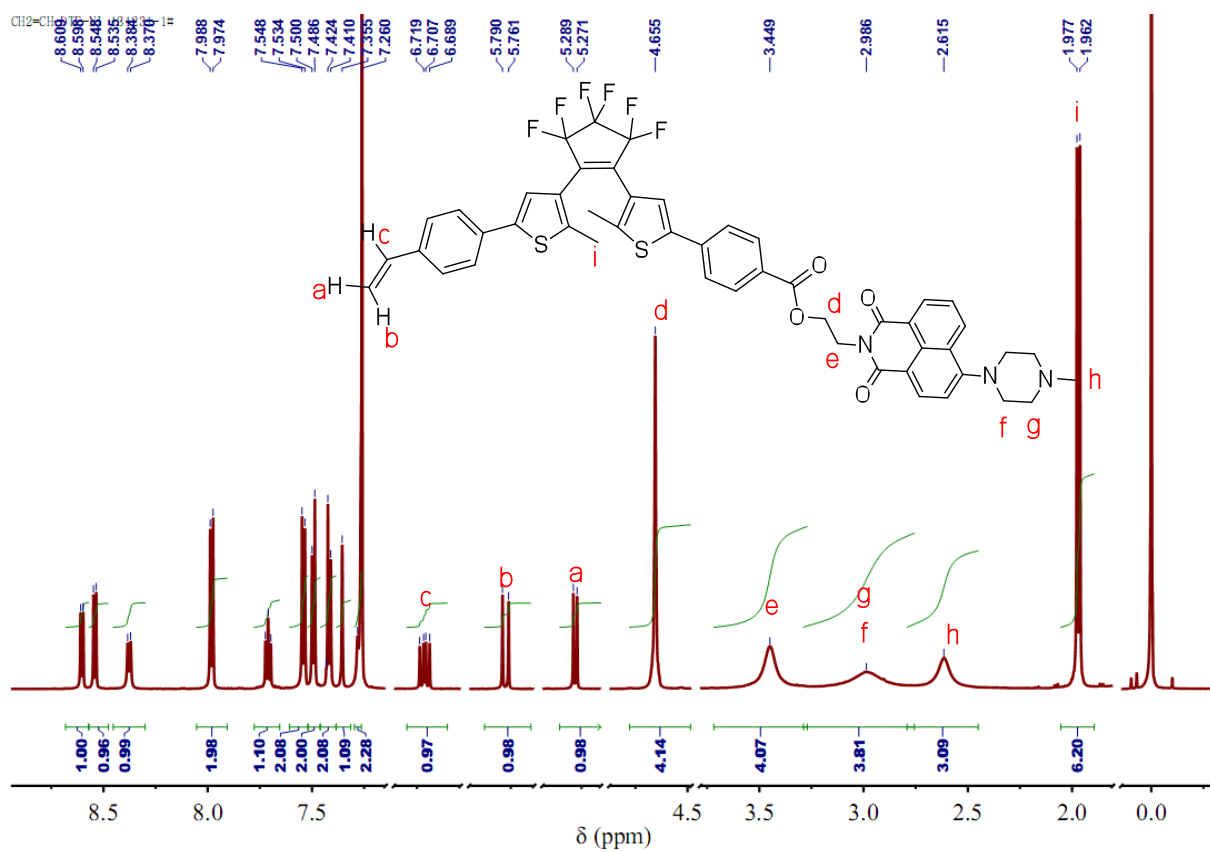
**Figure S15.** The HOMO and LUMO energy levels of compound **8** (model **DTE**) and compound **9** (model **NI**) computed using the B3LYP/6-31G(d) basis set.

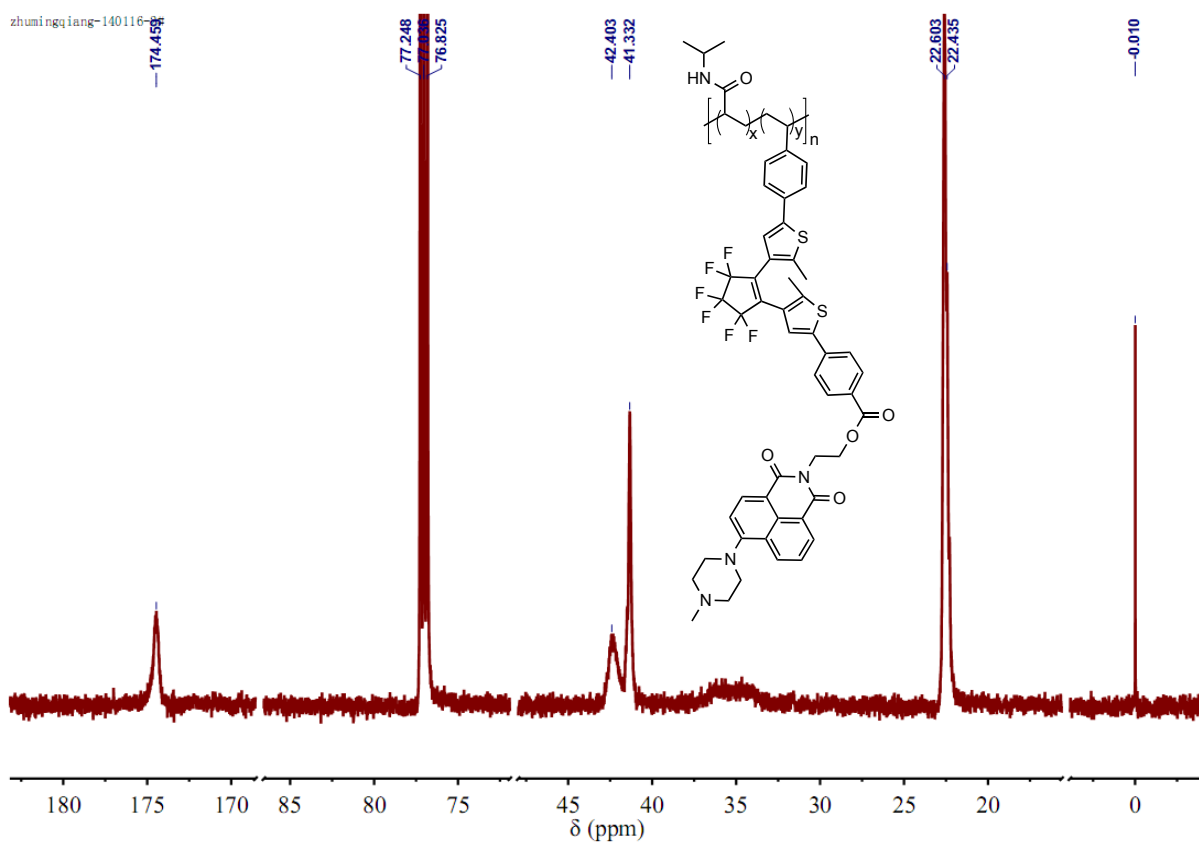
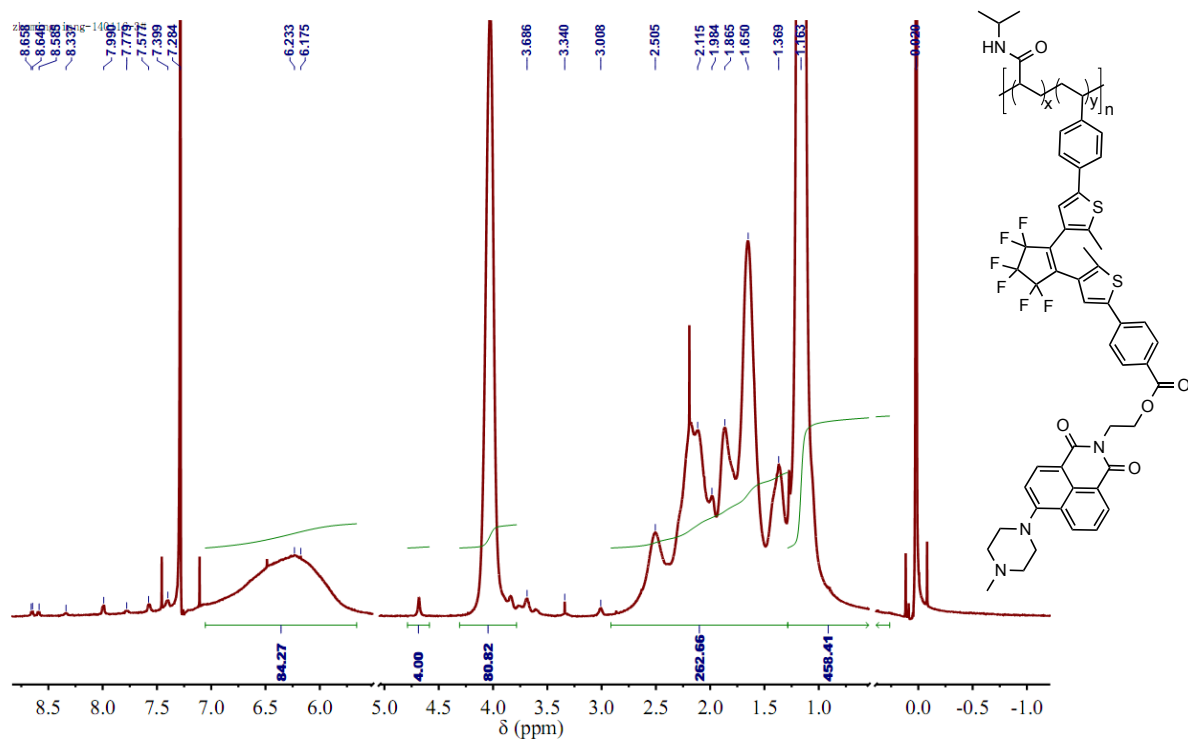


## 9. NMR SPECTRA.

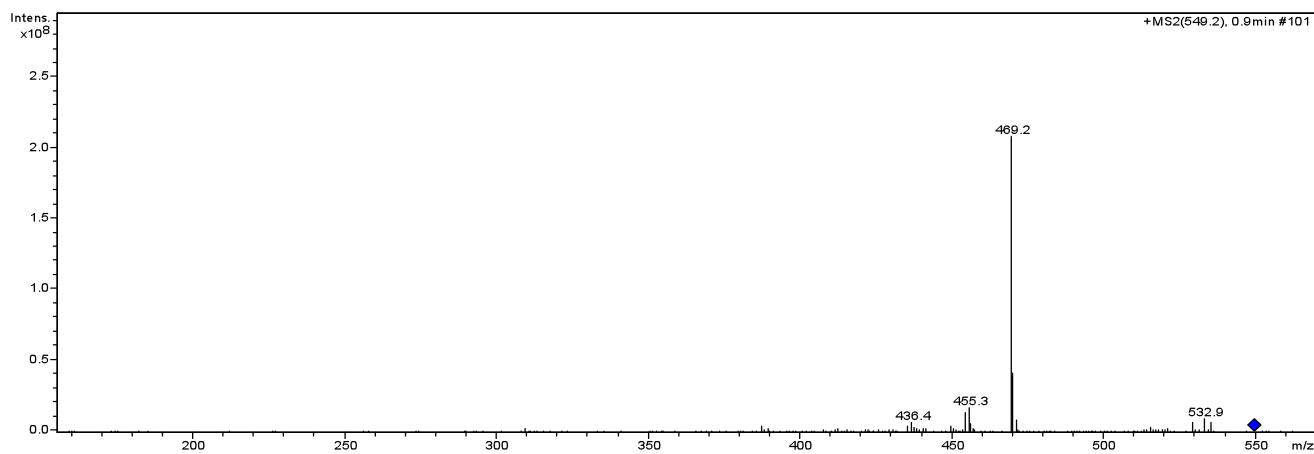
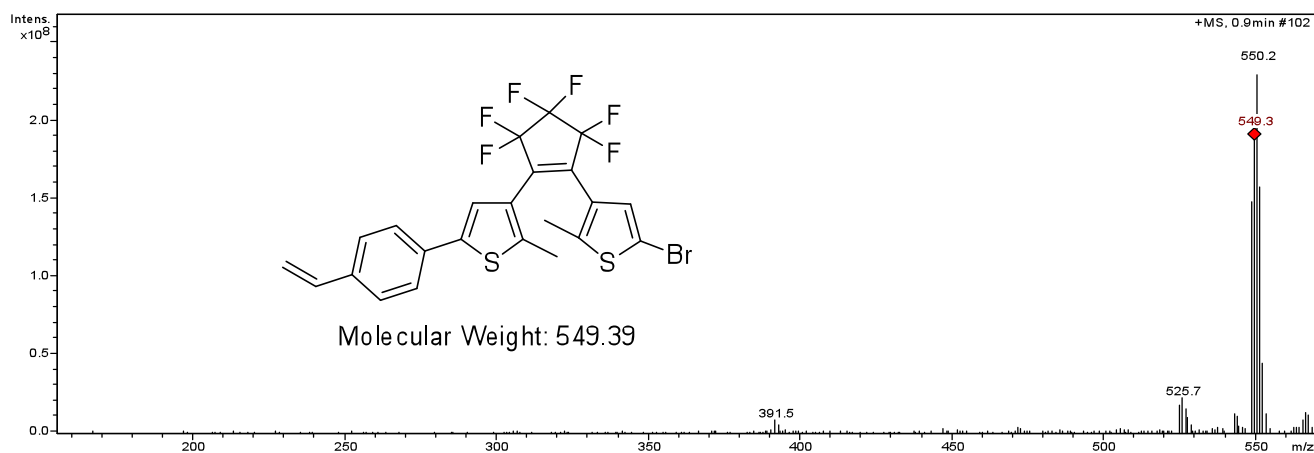


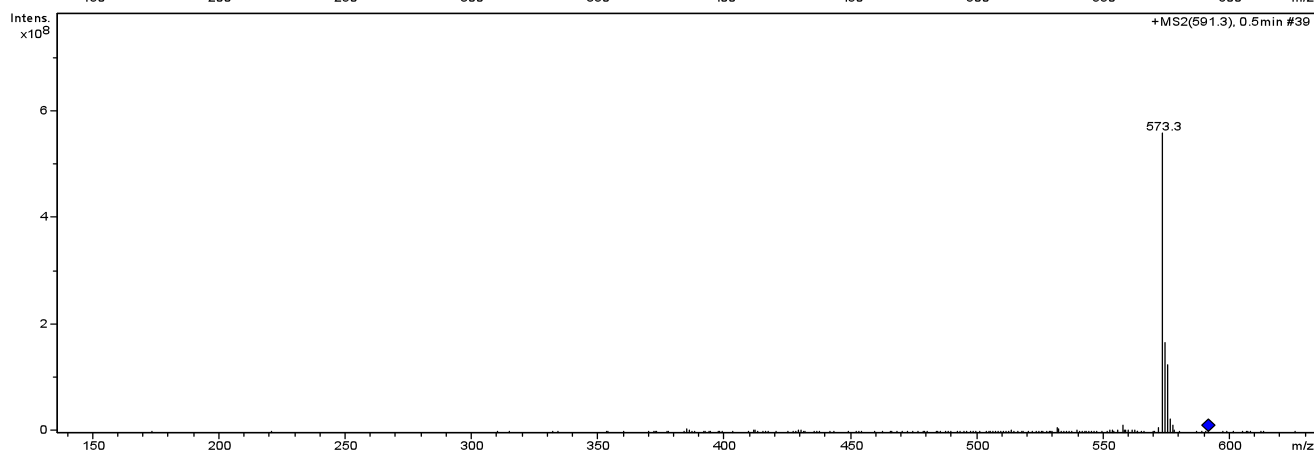
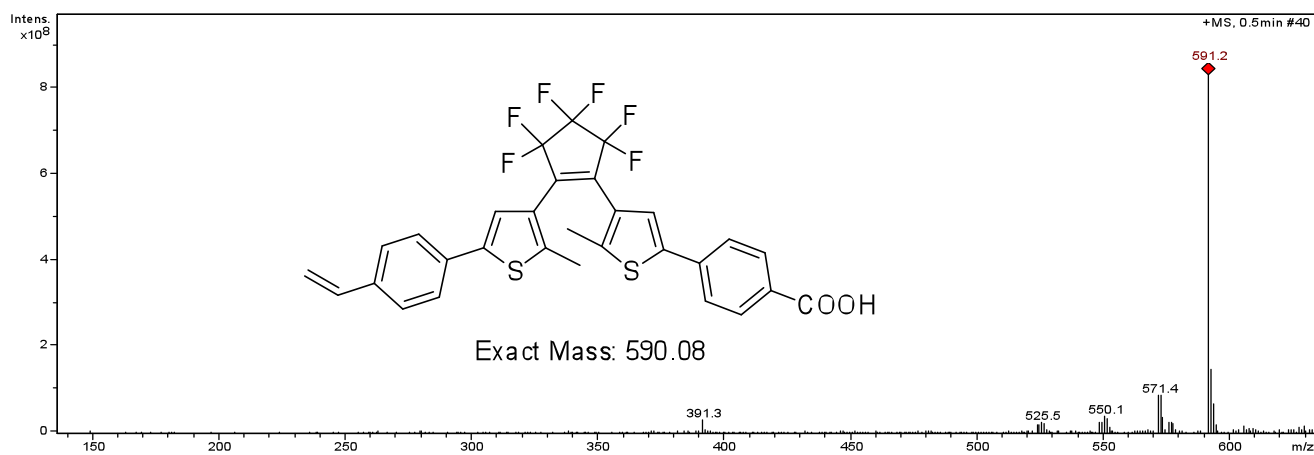


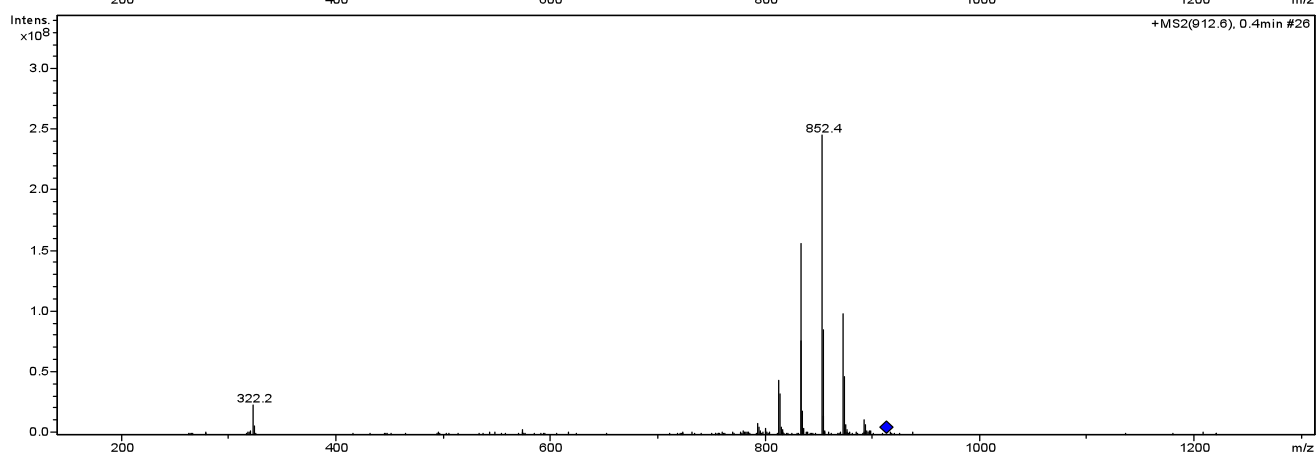
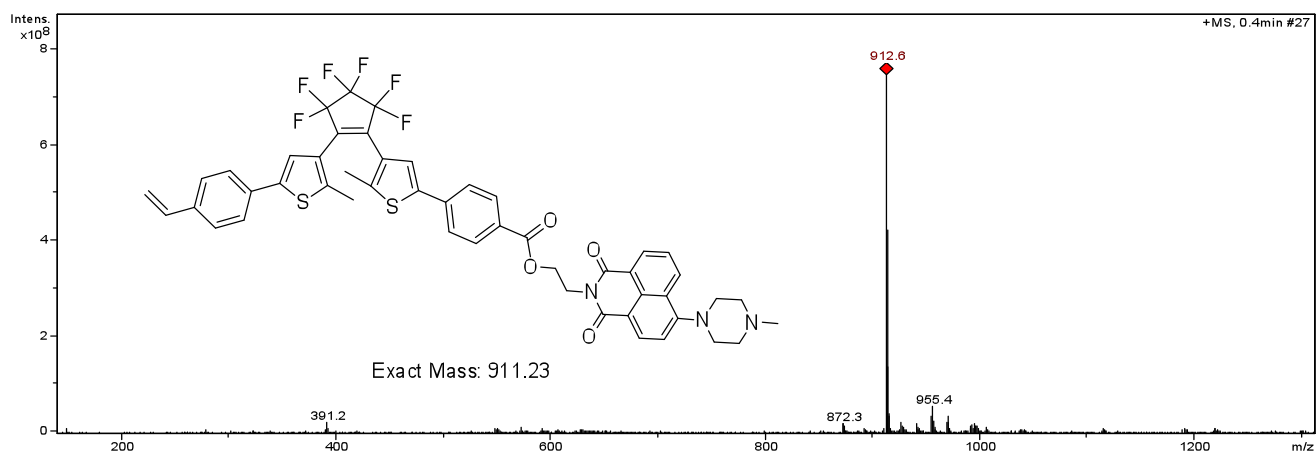




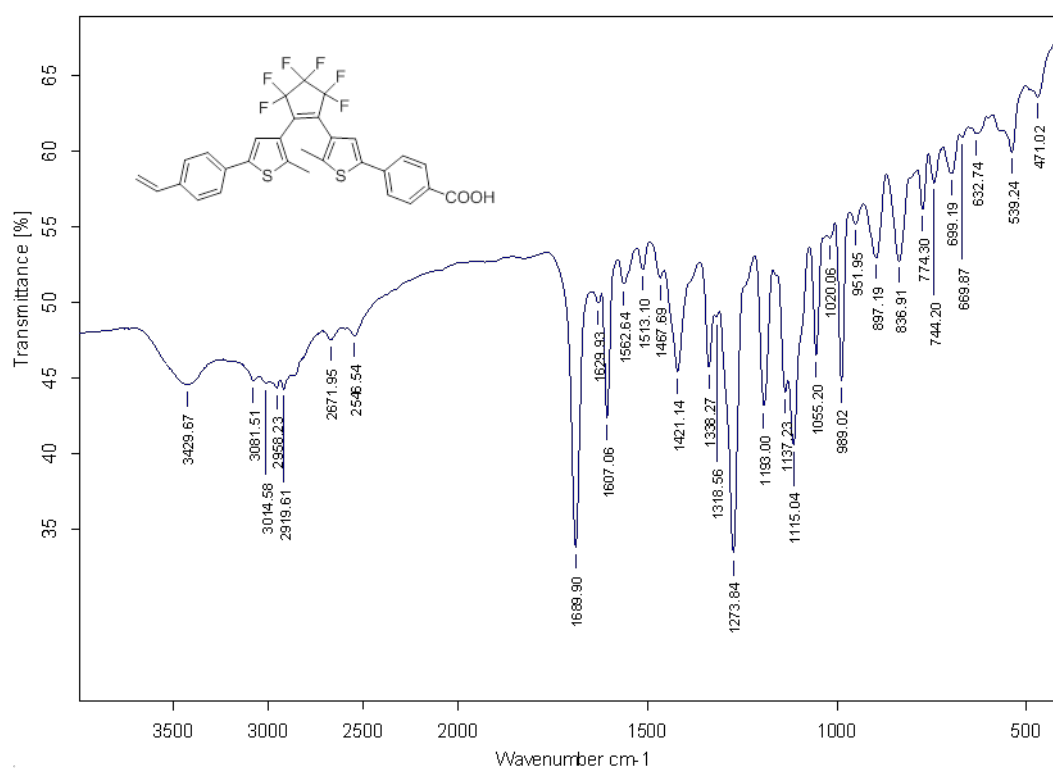
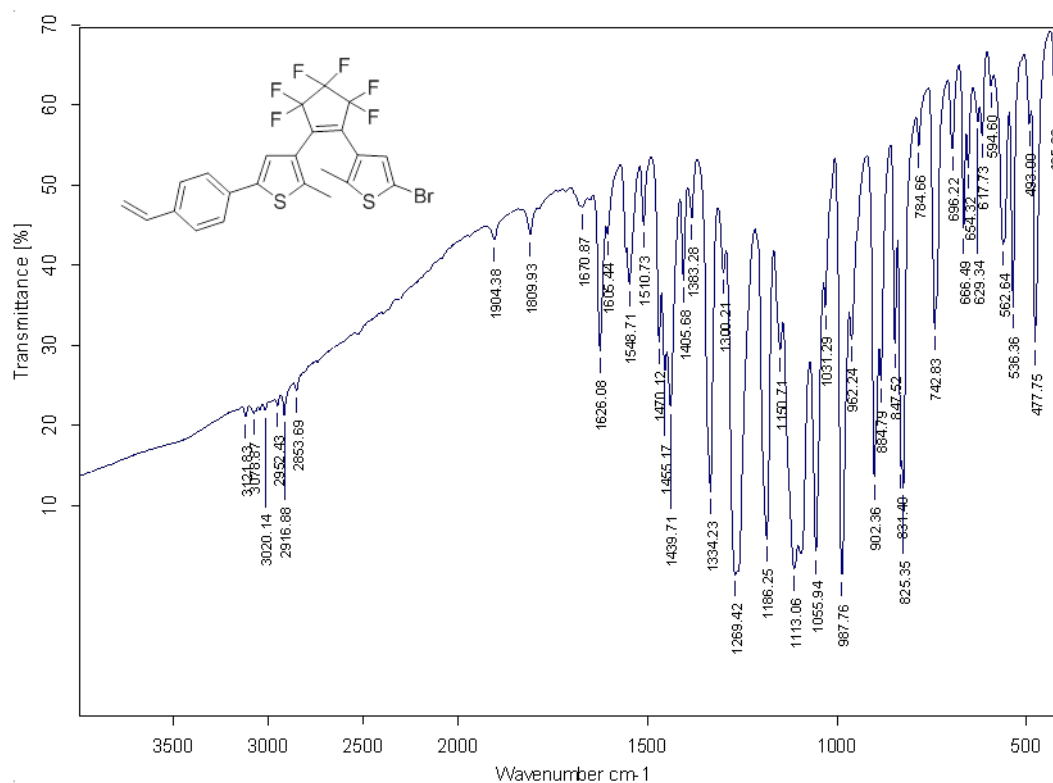
## 10.MASS SPECTRA.



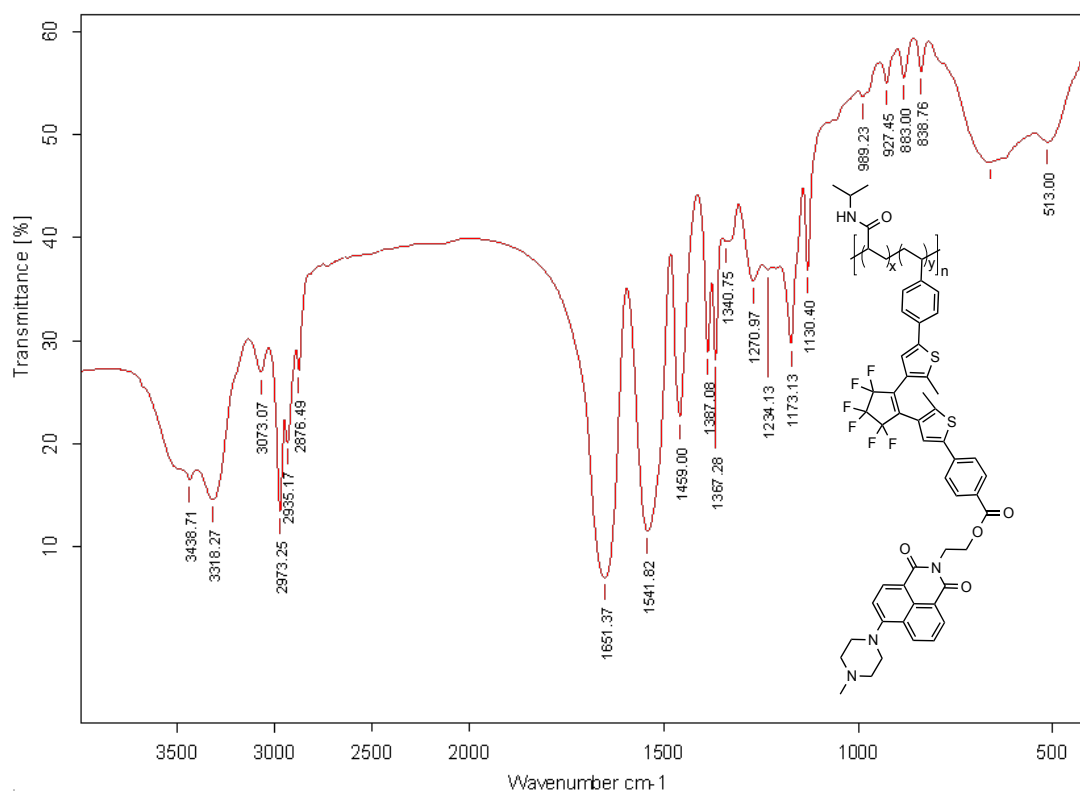
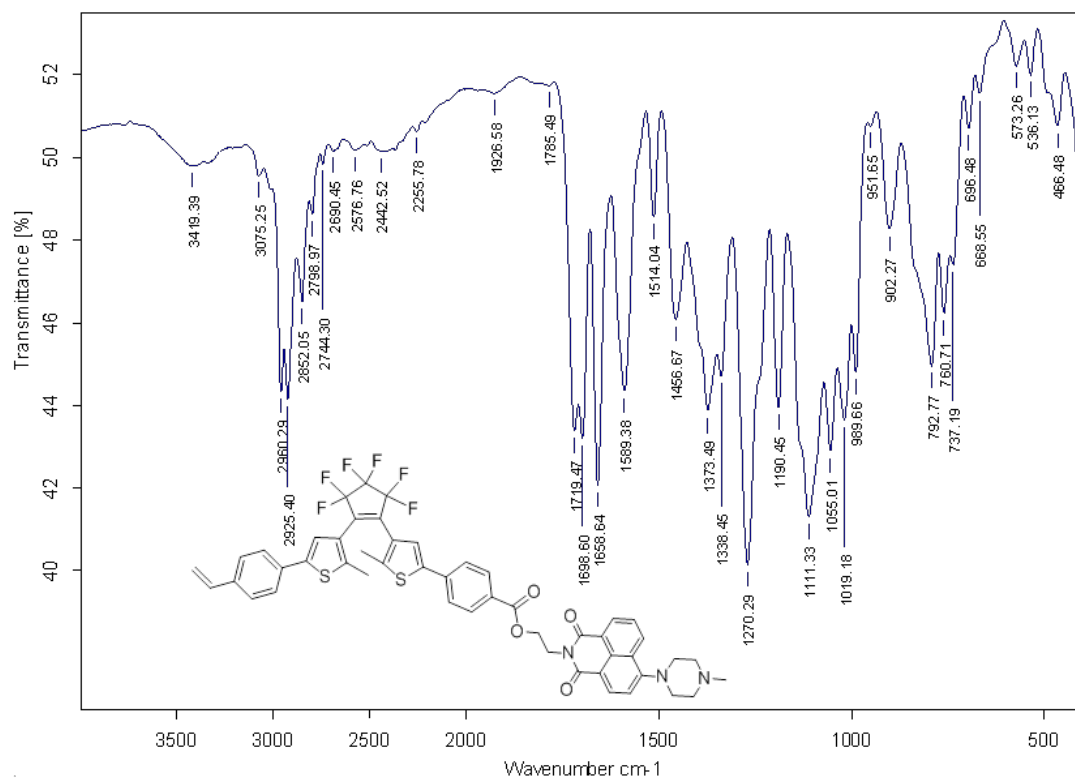




## 11. IR SPECTRA.







## REFERENCES.

1. Rurack, K.; Spieles, M. *Anal. Chem.* **2011**, 83, 1232–1242.